Journal of Experimental Botany, Vol. 64, No. 12, pp. 3669–3679, 2013
doi:10.1093/jxb/ert203
This paper is available online free of all access charges (see http://jxb.oxfordjournals.org/open_access.html for further details)

Journal of Experimental Botany
www.jxb.oxfordjournals.org

RESEARCH PAPER

Isochorismate synthase 1 is required for thylakoid organization, optimal plastoquinone redox status, and state transitions in *Arabidopsis thaliana*

Piotr Gawroński[1,*], Magdalena Górecka[1,*], Magdalena Bederska[2], Anna Rusaczonek[1], Ireneusz Ślesak[1,3], Jerzy Kruk[4] and Stanisław Karpiński[1,†]

[1] Department of Plant Genetics, Breeding and Biotechnology, Faculty of Horticulture, Biotechnology and Landscape Architecture, Warsaw University of Life Sciences-SGGW, Nowoursynowska 159, Warsaw, 02-776 Poland
[2] Department of Botany, Faculty of Agriculture and Biology, Warsaw University of Life Sciences-SGGW, Nowoursynowska 159, Warsaw, 02-776 Poland
[3] Institute of Plant Physiology, Polish Academy of Sciences, Niezapominajek 21, Kraków, 30-239 Poland
[4] Department of Plant Biochemistry and Physiology, Faculty of Biochemistry, Biophysics and Biotechnology, Jagiellonian University, Gronostajowa 7, 30-387 Kraków, Poland

* These authors contributed equally to this work.
† To whom correspondence should be addressed. E-mail: stanislaw_karpinski@sggw.pl

Received 10 January 2013; Revised 9 May 2013; Accepted 5 June 2013

Abstract

Isochorismate synthase 1 (ICS1) is a crucial enzyme in the salicylic acid (SA) synthesis pathway, and thus it is important for immune defences. The *ics1* mutant is used in experiments on plant–pathogen interactions, and ICS1 is required for the appropriate hypersensitive disease defence response. However, ICS1 also takes part in the synthesis of phylloquinone, which is incorporated into photosystem I and is an important component of photosynthetic electron transport in plants. Therefore, photosynthetic and molecular analysis of the *ics1* mutant in comparison with wild-type and SA-degrading transgenic NahG *Arabidopsis thaliana* plants was performed. Photosynthetic parameters in the *ics1* mutant, when compared with the wild type, were changed in a manner observed previously for state transition-impaired plants (STN7 kinase recessive mutant, *stn7*). In contrast to *stn7*, deregulation of the redox status of the plastoquinone pool (measured as 1–q_p) in *ics1* showed significant variation depending on the leaf age. SA-degrading transgenic NahG plants targeted to the cytoplasm or chloroplasts displayed normal (wild-type-like) state transition. However, *ics1* plants treated with a phylloquinone precursor displayed symptoms of phenotypic reversion towards the wild type. *ics1* also showed altered thylakoid structure with an increased number of stacked thylakoids per granum which indicates the role of ICS1 in regulation of state transition. The results presented here suggest the role of ICS1 in integration of the chloroplast ultrastructure, the redox status of the plastoquinone pool, and organization of the photosystems, which all are important for optimal immune defence and light acclimatory responses.

Key words: Chlorophyll fluorescence, photosynthetic electron transport (PET), phylloquinone, plastoquinone pool (PQ pool), salicylic acid (SA), state transitions (ST).

Introduction

One of the key factors affecting photosynthesis in the natural environment is the amount of available light. Plants possess the natural capacity to absorb light energy in excess of what is sufficient for photochemistry; thus, in full sunlight, only a portion of the light energy absorbed by chlorophylls is used for CO_2 fixation (Asada, 1999; Ruban *et al.*, 2004). The

quantity of absorbed light energy that exceeds the amount needed for photochemistry is referred to as excess excitation energy (EEE). EEE must be dissipated through both fluorescence and heat. The failure to dissipate and quench EEE is highly damaging to plants, and often leads to chlorosis, bleaching, or bronzing of leaves due to imbalanced reactive oxygen species (ROS) and hormonal cellular homeostasis (Karpinski *et al*., 1999; Niyogi, 1999; Apel and Hirt, 2004; Ruban *et al*., 2004; Laloi *et al*., 2007; Van Breusegem *et al*., 2008; Muhlenbock *et al*., 2008; Li *et al*., 2009).

Non-photochemical quenching (NPQ) is a protective mechanism which, when it is in balance with the photochemical processes, ensures the optimal use of absorbed light energy for photochemistry with minimal damage due to, for example, heat and ROS generation, and foliar cell death induction (Mateo *et al*., 2004; Baker, 2008; Li *et al*., 2009; Szechynska-Hebda *et al*., 2010). It consists of state transition (ST), photoinhibition, and EEE dissipation. ST is a mechanism which allows absorbed light energy to be adequately distributed between two photosystems; thus photosynthesis is optimally efficient under variable light conditions. For decades, the molecular basis of this process was unknown, but recent experiments have demonstrated a key protein involved in the regulation of ST (Bellafiore *et al*., 2005; Pribil *et al*., 2010; Shapiguzov *et al*., 2010). STN7 is a kinase that is crucial for phosphorylation of the mobile antenna, light-harvesting complex II (LHCII), during ST. Phosphorylated LHCII (e.g. in low light conditions) migrates to photosystem I (PSI) and enhances its light energy absorption—this is called state 2. In the case of PSI-favouring conditions (e.g. far-red light), LHCII is dephosphorylated by phosphatase PPH1/TAP38 and joins PSII (state 1), which results in a more efficient energy transfer to PSII. This process lasts a few minutes (Bellafiore *et al*., 2005; Pribil *et al*., 2010; Shapiguzov *et al*., 2010). Furthermore, the role of ST in the regulation of Darwinian fitness in field conditions was reported and confirmed (Frenkel *et al*., 2007).

However, an energy imbalance may also be compensated by plants in a different manner. During long-lasting non-optimal light conditions, plants adjust the number of reaction centres, LHCs, and the ratio of photosystems (Chow *et al*., 1990; Pfannschmidt *et al*., 1999). This takes at least a few hours, is more noticeable after a few days, and is called the long-term response (LTR). ST and LTR changes are brought about by modifications of the redox state of the plastoquinone (PQ) pool as well as PSI and PSII protein expression modifications, and lead to an alteration of the ultimate proportion of chlorophyll *a* and *b* (Pfannschmidt *et al*., 2001; Brautigam *et al*., 2009). It is also believed that the redox status of the PQ pool regulates immune defences, cell death, and light acclimatory responses induced by EEE conditions (Mateo *et al*., 2004; Muhlenbock *et al*., 2008; Szechynska-Hebda *et al*., 2010; Karpinski *et al*., 2013).

The role of the hormone salicylic acid (SA) in plant defence has been well studied (Loake and Grant, 2007; Vlot *et al*., 2009; An and Mou, 2011). The ROS burst drives the local accumulation of SA in cells surrounding the infection sites to induce defence and transcription of antioxidant genes. Loss of SA accumulation suppresses immune defences (Aviv *et al*., 2002), and it is widely accepted that SA is the main player in the regulation of cell death (Coll *et al*., 2011; Karpinski *et al*., 2013). However, SA is not only important for regulation of biotic stress responses. It has been shown that SA signalling is induced during light acclimatory responses and EEE dissipation, and that SA has a regulatory effect on photosynthesis, stomatal conductance, and cell death during light acclimation (Karpinski *et al*., 2003; Mateo *et al*., 2004; Muhlenbock *et al*., 2008). Additionally, SA is involved in physiological and molecular processes, such as the regulation of flowering or thermogenesis (Clarke *et al*., 2004; Vlot *et al*., 2009). These observations suggest that SA synthesis could regulate the cross-talk between light acclimatory and immune defence responses in plants.

There are at least two pathways of SA production in plants. In the first metabolic pathway, ~5% of SA is synthesized from benzoic acid by benzoic acid-2-hydrolase. In the second pathway, isochorismate plays a key role, and up to 95% of SA originates from this pathway (Vlot *et al*., 2009). There are two genes encoding isochorismate synthase (ICS), named *ICS1* and *ICS2*, in *Arabidopsis*. ICS catalyses isochorismate formation from chorismate (Garcion *et al*., 2008). Previous analyses indicate that *ics1* (also called *salicylic acid induction deficient 2*, *sid2*) is the main source of isochorismate, while the *ics2* null mutant does not have significantly decreased levels of SA (Garcion *et al*., 2008). Isochorismate is also a precursor of phylloquinone, known as vitamin K_1, which is a secondary electron acceptor from PSI and transfers an electron to the iron–sulphur cluster. The double null *ics1*/*ics2* mutant is pale green, smaller than the wild type (WT), and is totally devoid of phylloquinone (Garcion *et al*., 2008). This suggests that this pathway of phylloquinone biosynthesis is the only one in *Arabidopsis*.

Based on the information presented above, the following hypotheses have been formulated: (i) phylloquinone (PQ) as a PSI component could be involved in the regulation of ST through SA or the phylloquinone synthesis pathway; and (ii) ICS1 might play an important role in maintaining the balance between photosystems in variable light conditions.

Materials and methods

Plant material and growth condition

All plants used in this study were derived from the Col-0 ecotype. The *ics1* mutant, NahG, RbsC–NahG, and RbsC–NahG–green fluorescent protein (GFP) (RbsC is a chloroplast-targeting sequence) transgenic lines were described earlier (Gaffney *et al*., 1993; Wildermuth *et al*., 2001; Fragnière *et al*., 2011). The *stn7* mutant with impaired STs was described in Bonardi *et al*. (2005). Plants were grown for 4–5 weeks in Jiffy pots (Jiffy Products) in short-day conditions, 8 h light/16 h dark, at 22 °C under fluorescent white light: 80 µmol m^{-2} s^{-1}. If different growth conditions were applied, this is indicated in the text.

Chlorophyll a fluorescence measurements

Chlorophyll *a* fluorescence parameters were determined using a pulse amplitude-modulated FluorCam 800 MF PSI device (Brno, Czech Republic). The plants were kept in darkness for 30 min to

determine F_0 and F_m, exposed to 5 min of actinic red light (90 µmol m^{-2} s^{-1}) to determine F_t and F_m', then the actinic light was switched off and, after incubation with far-red light, F_0' was determined. The maximum quantum efficiency of PSII, $F_v/F_m=(F_m–F_o)/F_m$, non-photochemical quenching, NPQ=$(F_m–F_m')/F_m'$, photochemical quenching, $q_p=(F_m'–F_t)/(F_m'–F_0')$, and the operating quantum efficiency of PSII, ΦPSII=$(F_m'–F_s)/F_m'$ were determined as described earlier (Baker, 2008). Steady-state fluorescence (F_s) was calculated as $F_s=F_t–F_0'$, and used to determine the F_s/F_m parameter, which reflects the structural differences in the photosynthetic apparatus (Pfannschmidt *et al*., 2001). ST was determined on whole rosettes with a pulse amplitude-modulated FluorCam 800 MF device. F_0 was determined on dark-acclimated whole plants, then a 1 s flash of saturating light was applied to determine F_m. Plants were pre-illuminated with both blue (PSII light) and far-red light (PSI light) for 5 min, and subsequently only blue light (PSII light) was switched on for 15 min. The far-red light was turned on for 15 min and the maximum fluorescence in state 1 was determined (F_{m1}). Next, the far-red light was turned off and fluorescence was monitored for 15 min, after which the maximum fluorescence in state 2 was determined (F_{m2}). F_i and F_{ii} indicate fluorescence in the presence of PSI light in state 1 and state 2, respectively. F_i' and F_{ii}' denote fluorescence in the absence of PSI light in state 1 and state 2, respectively. The q_T and q_S parameters were calculated as $[(F_{m1}–F_{m2})/F_{m1}]$ and $[(F_i'–F_i)–(F_{ii}'–F_{ii})]/(F_i'–F_i)$, respectively (Damkjaer *et al*., 2009).

Phylloquinone determination

Phylloquinone was determined by the method of van Oostende *et al*. (2008) with the following modifications: the zinc post-column was 1 × 0.4 cm, and the solvent was methanol containing 10 mM $ZnCl_2$, 5 mM sodium acetate and 5 mM acetic acid. The fluorescence detection was performed at 245 nm excitation and 430 nm emission (Kruk *et al*., 1994).

Feeding with the precursor of phylloquinone

To check the role of phylloquinone in ST, 3-week-old *ics1* plants were sprayed with 100 µM 1,4-dihydroxy-2-naphthoic acid (NA; Sigma-Aldrich) in 0.2% dimethylsulphoxide (DMSO; Sigma-Aldrich) with 0.1% Tween-20 (Sigma-Aldrich) for 2 weeks, three times a week. Control *ics1* plants were treated with an analogous solution without NA. Adequate experiments on WT plants were conducted.

Sample preparation for light and transmission electron microscopy

Segments from the mid-lamina regions of mature, low light-acclimated (state 2-favouring conditions) leaves were cut from the Col-0 as the WT and from *ics1* plants directly into cold Karnovsky's fixative (Karnovsky, 1965). The segments were fixed for 2 h under a slight vacuum at room temperature. After 0.1 M cacodylate buffer rinses were repeated four times, the leaf tissue was post-fixed in 2% OsO_4 for 4 h. Subsequently, it was dehydrated through a cold ethanol series (10–100%), followed by several changes of propylene oxide, embedded in resin Epon 812 (Fluka), and polymerized for 24 h at 60 °C. Sections (3 µm) were cut onto glass slides using microtomes (Jung RM 2065 and Ultracut UCT, Leica), mounted in methylene blue and azure A, and examined using an Olympus AX70 Provis light microscope. Ultrathin sections were collected on copper grids and stained with uranyl acetate, followed by lead citrate for 1 min, and examined under a Morgagni 268C (FEI) transmission electron microscope.

Gas exchange and chlorophyll fluorescence analysis

Photosynthetic parameters in variable light conditions were measured using the Gas Exchange Fluorescence System GFS-3000 (Walz GmbH, *Effeltrich,* Germany) and calculated according to the manufacturer's instructions and Wituszyńska *et al*. (2013). Three-week-old plants cultivated at 120 µmol m^{-2} s^{-1} were examined.

Chlorophyll a/b ratio measurement

Four-week-old *Arabidopsis* plants were frozen in liquid nitrogen and 50–100 mg of frozen tissue was homogenized in a TissueLyser LT (Qiagen) (5 min; 50 s^{-1}, 4 °C) with 1 ml of cold acetone (–20 °C). The homogenate was evaporated under a nitrogen stream, dissolved in cold solvent A (acetonitrile:methanol; 90:10 v/v), and re-homogenized for 1 min. The extract was filtered through a syringe filter (0.2 µm nylon filter, Whatman) into an autosampler vial, capped, and stored in the dark at –80 °C until HPLC analysis (Shimadzu Liquid Chromatography System). Pigments were separated on a Synergi 4u MAX-RP 80A 250 × 4.6 column (Phenomenex) at 30 °C. A low-pressure gradient method was used: solvent A for 10 min, followed by solvent B (methanol:ethyl acetate; 68:32 v/v) for 10 min at a flow rate of 1 ml min^{-1}. Absorbance spectra were recorded at 440 nm by diode array detector. Pigments were identified by using standards obtained from Sigma. The results were expressed as a chlorophyll a/*b* ratio.

Thermoluminescence (TL) measurements

TL measurements of detached leaves were performed with the thermoluminescence TL 200/PMT system (Brno, Czech Republic). After 2 min of dark adaptation at 20 °C, the leaves were cooled to –6 °C and excited with one or a multiple number of single-turnover flashes. Then the samples were warmed up to 65 °C at a heating rate of 0.5 °C s^{-1}, and TL light emission was measured.

Microarray analysis

In the present analysis, data from Affymetrix ATH1 GeneChips published by Behringer *et al*. (2011) and deposited in the Gene Expression Omnibus (GEO) with the number GSE25489 were used. The CEL files of non-treated Col-0 and *ics1* were downloaded. The data were pre-processed and analysed using R and Bioconductor software (Gentleman *et al*., 2004). The array intensities were normalized using gcrma from the simpleaffy package (Wilson and Miller, 2005). The limma package (Smyth, 2005) was used to compare the hybridization intensities of Col-0 and *ics1*. Up- and down-regulated genes in *ics1* were defined as those whose hybridization intensities were significantly higher or lower than in Col-0 ($P < 0.05$, Student's *t*-test). Gene ontology (GO) terms were retrieved from the TAIR website (http://arabidopsis.org).

Analyses of quantum efficiencies of PSI

To examine the activity of PSI P700, absorbance changes at 830 nm and 875 nm were measured using a Dual-PAM-100 (Walz GmbH). The experiments were performed on the fifth to seventh detached leaves which had been dark adapted for a minimum of 30 min. Both slow kinetics and the light curve were determined. The parameters of PSI activity were calculated as described both by the manufacturer and by Niewiadomska *et al*. (2011). Moreover, the cyclic electron flow around PSI, $Y_{CEF}=Y_{(I)}–Y_{(II)}$, was calculated as described earlier (Miyake *et al*., 2005).

Results

Inhibition of state transitions in ics1 *is phylloquinone dependent*

To investigate the role of *ICS1* in the regulation of photosynthesis in *Arabidopsis*, chlorophyll *a* fluorescence in the

ics1 mutant and the WT plants was tested. The maximum quantum yield of photosystem II (F_v/F_m) was similar in *ics1* to that in the WT (Table 1). However, upon illumination with actinic light, the *ics1* plants were unable to quench chlorophyll *a* fluorescence (Fig. 1a), which is reflected in the increased F_s/F_m parameter (Table 1), indicating that perturbations in photosynthesis may be located beyond PSII. The PQ pool was more reduced in plants lacking *ICS1*, as indicated by the $1–q_p$ value (Table 1). To check if the *ics1* plants had an impaired mechanism of ST, changes of chlorophyll *a* fluorescence in state 1- and state 2-favouring light conditions were investigated (Fig. 1a). Transitions from state 1 to state 2 can be described by the q_T and q_S parameters (as described in the Materials and methods). The q_T value in the WT plants was 0.114 ± 0.006, while in *ics1* it was decreased to 0.037 ± 0.003. Similarly, the q_S value in the WT plants was 0.883 ± 0.006, while in *ics1* it was decreased to 0.549 ± 0.002 (Table 1). To test if perturbation in ST in *ics1* was due to strongly diminished SA levels, the chlorophyll *a* fluorescence parameters were measured in transgenic NahG plants carrying a bacterial gene encoding salicylate hydroxylase (which converts SA to the catechol) localized in the cytosol and in the chloroplast. However, neither plants with a cytosolic localization of NahG nor those with chloroplast-targeted NahG demonstrated ST disorders (Fig. 1b). Therefore, the role of SA in ST was excluded. The analysis of the phylloquinone content showed that the content of phylloquinone in the *ics1* mutant was 55% of that in the WT when calculated on a fresh weight (FW) basis, and 58% of that of the WT in relation to chlorophyll (Table 1). The obtained results are similar to, although higher than, those reported by Garcion *et al.* (2008) where the phylloquinone content (per g FW) in the mutant was 35% of the value found for the WT. To examine if the observed ST alterations in *ics1* were due to a depleted phylloquinone synthesis pathway (another metabolic pathway dependent upon ICS1 activity), the *ics1* plants were treated with the precursor of phylloquinone, NA. Two weeks of systematic treatment with NA significantly increased q_T in the *ics1* plants from 0.037 ± 0.003 to 0.102 ± 0.002, and q_S from 0.549 ± 0.002 to 0.743 ± 0.003 (Fig. 1c, Table 1). No significant changes in ST in NA-treated WT plants in comparison with the non-treated WT plants were observed (Fig. 1c, Table 1).

Table 1. *Photosynthetic parameters of WT and* ics1 *plants*

	WT	*ics1*
F_s/F_m	0.048 ± 0.008 (*n*=6)	0.110 ± 0.009 (*n*=6)
$1–q_P$	0.088 ± 0.004 (*n*=6)	0.200 ± 0.015 (*n*=6)
F_v/F_m	0.847 ± 0.010 (*n*=6)	0.842 ± 0.016 (*n*=6)
NPQ	0.445 ± 0.113 (*n*=6)	0.407 ± 0.105 (*n*=6)
Chl *a*/*b*	2.70 ± 0.09 (*n*=7)	2.50 ± 0.07 (*n*=5)
Phylloquinone (μg g FW^{-1})[a]	5.62 ± 0.55 (*n*=5)	3.07 ± 0.64 (*n*=5)
Phylloquinone (mol 100 mol^{-1} Chl)[a]	1.04 ± 0.07 (*n*=5)	0.60 ± 0.10 (*n*=5)
q_T	0.114 ± 0.006 (*n*=6)	0.037 ± 0.003 (*n*=6)
q_T (+NA)[b]	0.116 ± 0.010 (*n*=6)	0.102 ± 0.002 (*n*=6)
q_S	0.883 ± 0.006 (*n*=6)	0.549 ± 0.002 (*n*=6)
q_S (+NA)[b]	0.880 ± 0.005 (*n*=6)	0.743 ± 0.003 (*n*=6)
Y_{CEF}	0.23 ± 0.03 (*n*=8)	0.34 ± 0.04 (*n*=8)

Values are means ±SD.
[a] The experiment was repeated twice with similar results.
[b] Values for plants sprayed with NA (for details, see the Materials and methods).

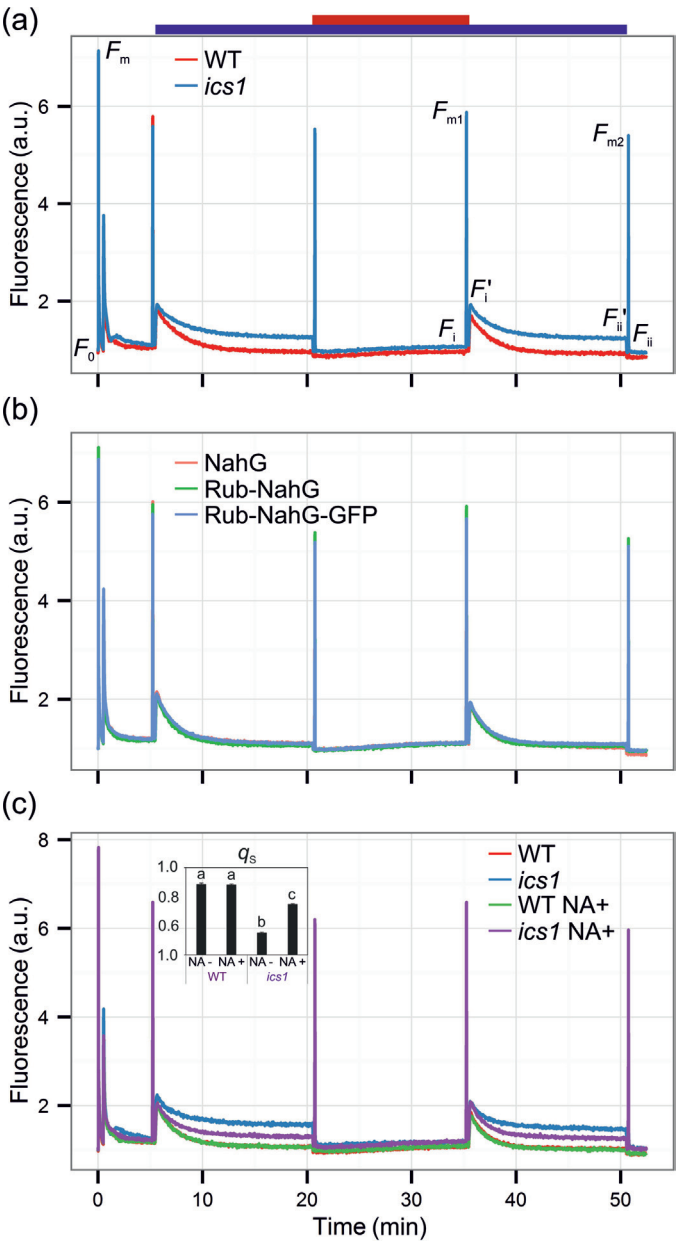

Fig. 1. State transition in wild-type and *ics1* plants (a), NahG transgenic plants with both a cytosolic- and chloroplast-targeted SA-degrading enzyme (b), and wild-type and *ics1* plants supplemented with the phylloquinone precursor (1,4-dihydroxy-2-naphthoic acid; NA) (c). The top bar depicts lights applied during a particular period of the measurement; blue, actinic light on; red, far-red light on. The graph shows representative measurements of six whole rosettes for each genotype and treatment. The inset in (c) shows the q_S parameter (mean ±SD) for the analysed genotypes and treatments. Homogeneous groups were calculated using Tukey HSD analysis. For details, see the Materials and methods.

Transmission electron microscopy

Transmission electron microscopy was used to determine the organization of internal membranes in the chloroplasts of the WT and *ics1*. Thylakoid membranes were differentiated into two domains that were different morphologically and functionally, namely grana and unstacked (non-appressed) membranes called stroma lamellae. The grana were interconnected by the stroma thylakoids. The thylakoids were flattened and oriented towards the longitudinal axis of the thylakoid system. The large starch grains and a few and relatively small plastoglobuli were observed in the stroma (Fig. 2).

In general, the organization of the thylakoid membranes in the WT was similar to that observed in *ics1* (Fig. 2). However, observations revealed some differences. The *ics1* grana stacks had more thylakoids when compared with the chloroplasts from the WT. Moreover, the grana in *ics1* were rare in comparison with the WT chloroplasts. Although thylakoids form characteristic granum structures, an increased number of layers in the stacks can be seen in *ics1* (Fig. 2).

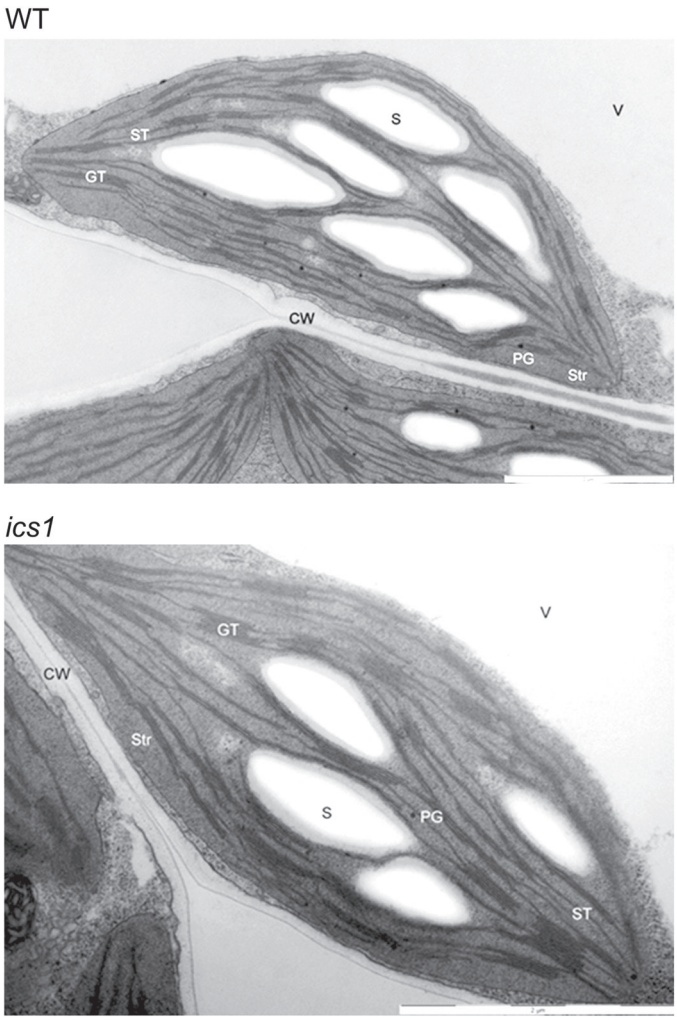

Fig. 2. Representative pictures of the chloroplast structure from WT and *ics1* plants. The WT chloroplasts show a typical structure with a lamellar system of granal and stromal thylakoids, while in *ics1* enlargement of the granum showing numerous stacked thylakoid sheets can be observed. CW, cell wall; GT, grana thylakoids; PG, plastoglobuli; S, starch; ST, stroma thylakoids; Str, stroma; V, vacuole. Bar=2 μm.

Photosynthetic parameters in ics1

To assay if the observed changes in fluorescence in the *ics1* mutant are due to alterations in the mechanisms of NPQ in the WT and *ics1*, the plants were grown at 120 μmol m^{-2} s^{-1} and the rosettes were challenged with increasing light intensities. No significant differences in NPQ between the *ics1* and WT plants were observed (Table 1; Supplementary Fig. S1a available at *JXB* online). In the *ics1* rosettes, the PQ pool, expressed as a $1–q_P$, was more reduced than in the WT plants (Table 1, Fig. 3a), while this difference was more pronounced at lower light intensities. The level of reduction of the PQ pool (expressed as $1–q_P$) in light-exposed *ics1* plants was significantly higher in young than in old, well-developed leaves and oscillates around values obtained for *stn7* that were similar in all leaves (Fig. 4). However, $1–q_P$ values in WT control plants were significantly lower than those in *ics1* and *stn7*, and were also homogeneous in the whole rosette (Fig. 4). Higher PQ pool reduction levels correlate with an increased yield of cyclic electron flow (Y_{CEF}) around PSI observed in *ics1* in comparison with the WT (Table 1). However, CO_2 assimilation in *ics1* was similar to that in the WT plants (Supplementary Fig. S1c). These data are consistent with the fact that there was no significant difference in growth between *ics1* and WT in laboratory conditions (Mateo *et al.*, 2006).

Thermoluminescence

TL was further used to investigate the redox properties of the acceptor and donor sides of PSII in the WT and *ics1* plants. In order to confirm that the redox state of the PQ pool is more reduced in the *ics1* mutants, the flash-induced patterns of TL in the WT and mutants were measured. The best characterized TL band is the B-band. Illumination of a single turnover flash with the plant sample after a short dark adaptation induces a major B-band, which appears at ~30–35 ºC (Misra *et al.*, 2001; Ducruet and Vass, 2009; Sane *et al.*, 2012). It is correlated with the activity of the oxygen-evolving complex (OEC). As is shown in Fig. 3b, the temperature peak for the TL glow curves was ~30–35 ºC, thus indicating that the B-band was responsible for TL emission in both the WT and *ics1* plants, but in the *ics1* plants the B-band amplitude (TL_{max}) was strongly decreased (Fig. 3b). When the B-band amplitude (TL_{max}) is plotted against the flash number, a periodicity-of-four oscillation is clearly seen, with maxima occurring on the second and sixth flashes (Fig. 3c; Inoue, 1996). When the dark-adapted PSII centre is exposed to a series of short turnover flashes, formation of the redox pairs: $S_2Q_B^-$, $S_2/S_3Q_B^-$, and $S_3Q_B^-$ is expected after one, two, and three flashes, respectively (Sane *et al.*, 2012). It was observed that after two turnover flashes, the transformation of the $S_2Q_B^-$ charge pairs

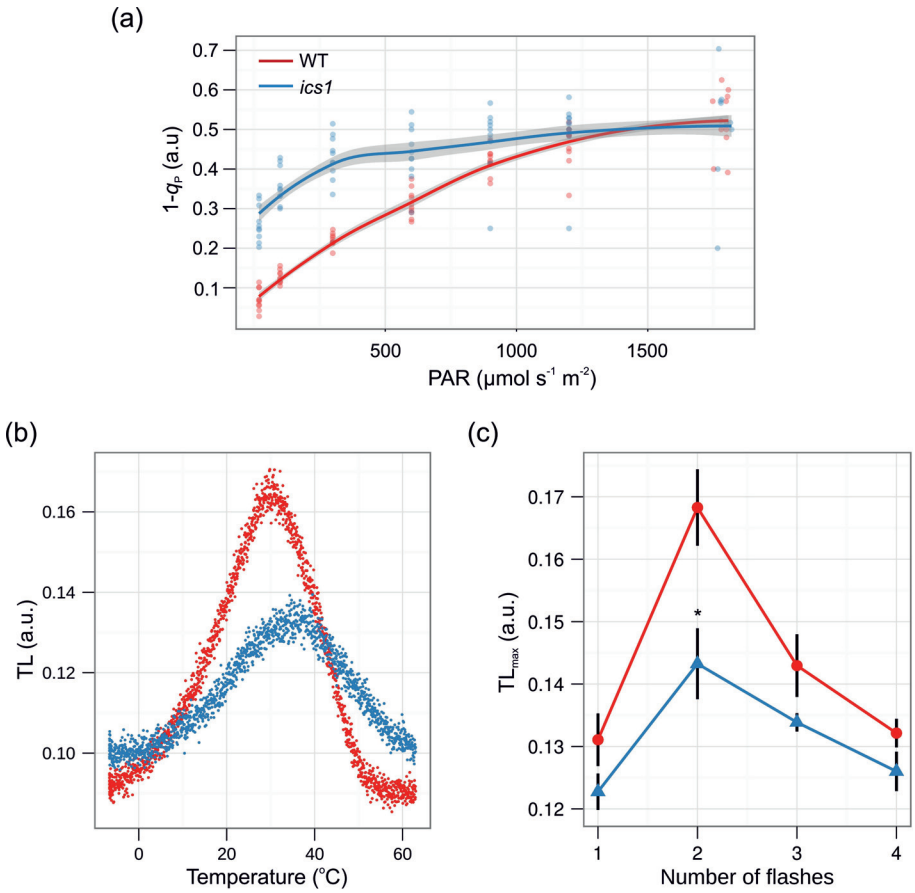

Fig. 3. Redox status of the plastoquinone pool. (a) Light curve of the redox status of the PQ pool ($1–q_P$). Data represent an average from 10 different rosettes (n=10, grey shading indicates the 95% confidence intervals for the analysed genotypes). (b and c) Thermoluminescence (TL) measurements. (b) TL glow curves in wild-type (WT, red dots) and *ics1* (blue dots) plants. The figure shows representative measurement of the leaves excited with two flashes. (c) Flash-induced oscillation of the B-band amplitude (TL_{max}) in wild-type (WT, red line and dots) and *ics1* (blue line and triangles) plants. Values are means ±SEM of seven independent measurements (leaves from seven independent plants). Asterisks indicate a significant difference from the control at $P < 0.05$ (according to Student's *t*-test).

to $S_2/S_3Q_B^-$ was inhibited in *ics1* in comparison with the WT (Fig. 3c). However, the oscillatory pattern of the B-band TL_{max} showed similar rhythmicity to that in the WT leaves (Fig. 3c).

Microarray analysis

The redox status of the PQ pool may influence the expression of nuclear and chloroplast genes (Escoubas *et al.*, 1995; Karpinski *et al.*, 1997, 1999; Pfannschmidt *et al.*, 1999, 2001; Muhlenbock *et al.*, 2008). To test whether the mRNA profile of the non-treated *ics1* mutant is different from that of the WT, publicly available microarray data (Behringer *et al.*, 2011), deposited in GEO (GSE25489), were analysed. The total number of differentially regulated genes at $P < 0.05$ (in comparison with the WT) in *ics1* was 1558. Of these, 773 were induced while 785 were inhibited in *ics1*. Interestingly, according to GO analysis, the protein products of genes induced in *ics1* are predicted to be predominantly targeted to the chloroplasts (33.2%) (Fig. 5a, b). Such an enhancement of the chloroplast-targeted proteins was not observed among the inhibited transcripts in *ics1* (8.3%) (Fig. 5a, b).

Efficiency of PSI in ics1

As the mutation in *ICS1* causes a deficiency of phylloquinone, it was expected that the efficiency of PSI in the *ics1* mutant would be decreased. However, the results show that there are no significant changes in the efficiency of PSI in *ics1* as compared with the WT plants (Supplementary Fig. S2 at *JXB* online). It is worth noting that there are slight differences in the yield of PSI [$Y_{(I)}$] and the acceptor-side limitation of PSI (Y_{NA}) (Supplementary Fig. S2). The donor-side limitation of PSI, Y_{ND}, does not seem to be affected in the *ics1* mutant (Supplementary Fig. S2).

Discussion

Two isochorismate synthase genes, *ICS1* (AT1G74710) and *ICS2* (AT1G18870), exist in the *Arabidopsis* genome. The protein products of these genes, ICS1 and ICS2, possess plastid-targeting signals and are indeed localized in the chloroplasts (Garcion *et al.*, 2008). ICS converts chorismate to isochorismate, which is a precursor of SA as well as phylloquinone

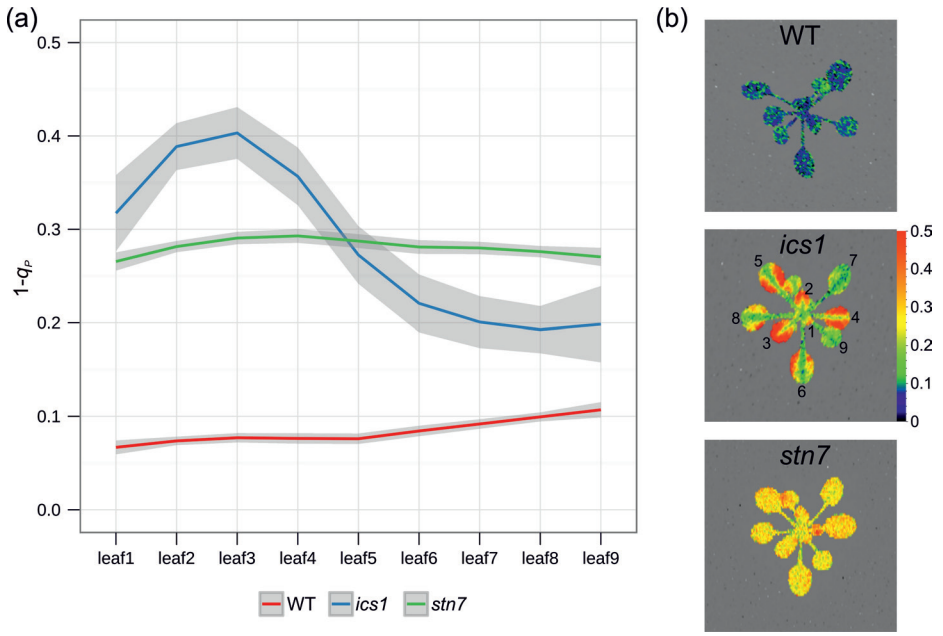

Fig. 4. Different patterns of the PQ pool reduction in *ics1*, *stn7*, and WT *Arabidopsis* rosettes. (a) The redox status of the plastoquinone pool (expressed as 1–q_p) in different leaves of *ics1*, *stn7*, and the WT. Data represent an average from six different rosettes (n=6; grey shading indicates the 95% confidence intervals for the analysed genotypes). (b) Photos show false-colour images of 1–q_p for *ics1*, *stn7*, and the WT.

(Gross *et al.*, 2006; Garcion *et al.*, 2008). In contrast to the SA synthesis pathway, ICS-dependent phylloquinone synthesis is the only known pathway of phylloquinone synthesis in *Arabidopsis*. However, *ics1* is commonly used as a model mutant with abolished SA synthesis, especially in experiments concerning plant pathogenesis (Wildermuth *et al.*, 2001; Ichimura *et al.*, 2006; Mishina and Zeier, 2007; Genger *et al.*, 2008; Chen *et al.*, 2009); the role of ICS1 in phylloquinone synthesis is often omitted. Therefore, the role of ICS1 in the regulation of photosynthesis, chloroplast membrane structure, and chloroplast to nucleus retrograde signalling was analysed.

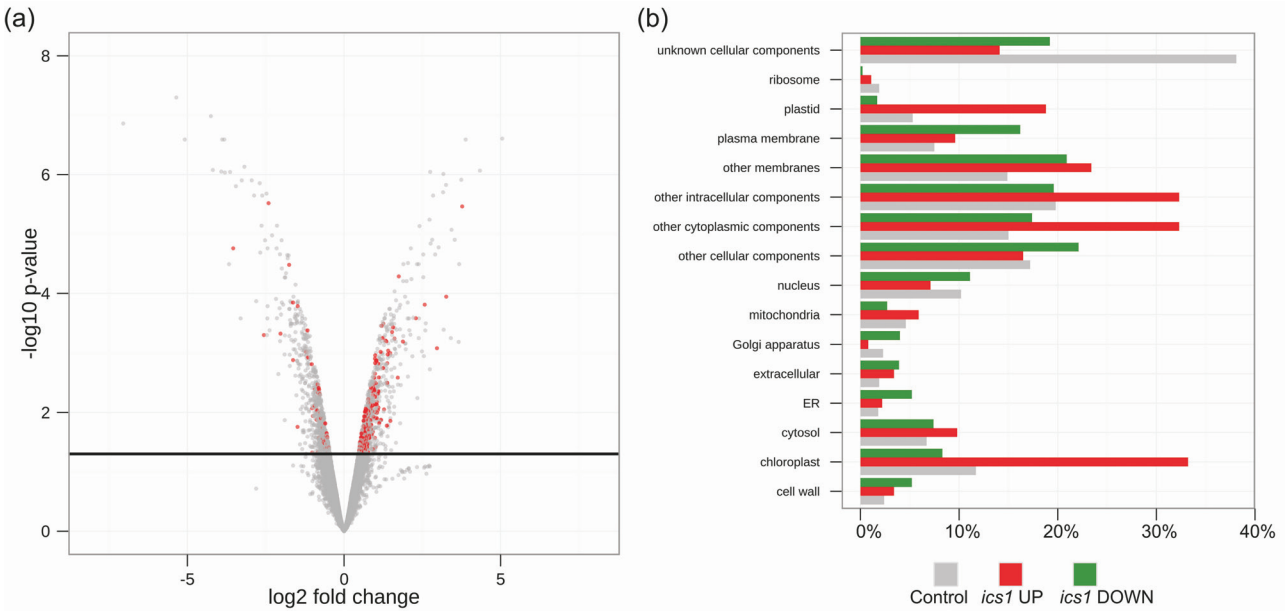

Fig. 5. Microarray analysis of the *ics1* mutant. (a) Volcano plot of microarray data. The log fold change is plotted on the *x*-axis (down-regulated genes on the left side, up-regulated on the right) and the negative log10 *P*-value is plotted on the *y*-axis. The black, solid line represents the *P*-value cut-off (0.05, Student's *t*-test). Points above the line have *P*-values <0.05 and points below the line have *P*-values >0.05. The red points represent genes whose protein products are targeted to the chloroplasts. (b) Gene ontology (Cellular Component) of genes induced (red) and suppressed (green) in *ics1*. As a control, whole-genome categorization (grey) was used.

To test if ICS1 influences ST, the changes of chlorophyll *a* fluorescence in light conditions which preferentially excite PSII (blue light) or PSI (blue light and far-red light) were measured (Fig. 1a). It was also shown that ST inhibition in *ics1* is phylloquinone dependent (Fig. 1c) and is not caused by a strongly decreased level of SA in *ics1* (Fig. 1b, c). The complete reversion of the q_T and q_S parameters in NA-treated *ics1* plants was not observed, possibly due to a limitation of the treatment (spraying 3-week-old plants which had already developed leaves could influence the measured parameters, which were averaged from whole rosettes). The results obtained from NahG-overexpressing plants (localized in the cytoplasm and the chloroplast) indicate that SA is not directly involved in the regulation of ST. Furthermore, it was found that the q_T and q_S values are significantly decreased in *ics1* (Table 1). To check whether the observed changes in fluorescence are due to impaired NPQ, the photosynthetic parameters were also measured in rosettes challenged with different light intensities. NPQ and CO_2 assimilation in WT and *ics1* plants were unaltered (Supplementary Fig. S1a, b at *JXB* online).

The results presented here prove that phylloquinone is an important element of the photosynthetic apparatus and not only plays a role in electron transfer through PSI, but is also essential for optimal energy distribution between photosystems. At present it cannot be asserted that the lack of phylloquinone causes conformational modifications of PSI so that it cannot bind the antennae complexes. It is also possible that due to efficient electron transfer through PSI, phylloquinone ensures an energetic equilibrium in both PSI and PSII and maintains the PQ pool in an optimally oxidized state. However, in PSI efficiency measurements for the *ics1* mutant, a slightly increased yield of PSI [$Y_{(I)}$] and a decreased acceptor side limitation (Y_{NA}) (Supplementary Fig. S2 at *JXB* online) were observed, which can be caused by an increased cyclic electron flow (CEF) around PSI (Table 1). These observations remain consistent with the measurements of the redox state of the PQ pool (expressed as $1–q_P$) in *ics1*, where PQ was more reduced than in the WT (Fig. 3a, Table 1). Variation in the PQ pool reduction levels between leaves in different developmental stages of *ics1* plants was observed, while in WT and *stn7* plants, the redox state of the PQ pool is independent of the leaf age (Fig. 4). This result suggests that the function of ICS1 is to stabilize the redox status of the PQ pool independently of the leaf age. This is required for optimization of immune defences and light acclimatory responses in the whole *Arabidopsis thaliana* rosette (Karpinski *et al*., 1999, 2013; Muhlenbock *et al*., 2008; Szechynska-Hebda *et al*., 2010).

Furthermore, glutathione reductase (GR) activity in *ics1* was decreased, and changes in foliar SA and reduced glutathione levels in *A. thaliana* were positively correlated (Mateo *et al*., 2006). Therefore, lowered GR activity could be explained by an increased NADPH consumption by the CEF (Munekage and Shikanai, 2005), which in turn may cause increased reduction of the PQ pool (Karpinska *et al*., 2000).

The redox status of the PQ pool is well known as an important regulator of integrated light acclimatory and immune defence processes, and retrograde signalling from the chloroplasts to the nucleus in plant cells (Escoubas *et al*., 1995; Karpinski *et al*., 1997, 1999, 2013; Pfannschmidt *et al*., 1999; Kruk and Karpinski, 2006; Muhlenbock *et al*., 2008; Rochaix, 2011). For instance, it regulates ST by activation/deactivation of kinase/phosphatase (Allen, 2003; Depège *et al*., 2003). To confirm deregulation in the redox state of the PQ pool in the *ics1* mutant, TL measurements were performed. TL originates from PSII via thermally stimulated delayed light which is emitted by singlet excited chlorophylls and generated by a recombination of the $S_2Q_A^-$, $S_2Q_B^-$, and $S_3Q_B^-$ charge pairs, where S_2 and S_3 denote the oxidation states of the manganese OEC and the primary (Q_A) and secondary (Q_B) quinone electron acceptors in PSII (Ducruet, 2003; Ducruet and Vass, 2009). The charge pairs involved can be identified by their emission temperatures, which strongly depend on the redox potentials of the charge pairs. It is assumed that the dark-adapted samples contain ~25% S_0 and 75% S_1, and the distribution of Q_B and Q_B^- has been shown to be 50:50 (Inoue, 1996). According to the previously described model (Inoue, 1996; Sane *et al*., 2012), in the dark-adapted samples the proportion of charge pairs is predicted as 25% $S_0/Q_B/Q_B^-$ and 75% $S_1/Q_B/Q_B^-$. After first saturating, the turnover flash Q_B is converted to Q_B^- and Q_B^- to Q_B^{2-}. After two-electron reduction, Q_B^{2-} is transformed into a protonated form (Q_BH_2), which is replaced by a new Q_B from the reoxidized PQ pool. After two turnover flashes, the TL signal originates predominantly from $S_3Q_B^-$ (the lower intensity of TL is also emitted by the $S_2Q_B^-$ charge pair) (Sane *et al*., 2012). The decreased amplitude of the B-band in the *ics1* mutant after two turnover flashes strongly suggests that the PQ pool which provides Q_B at the acceptor side of PSII (the quinone reduction cycle) is more reduced than in the WT (Fig. 3b, c). These results strongly support the measurements of chlorophyll *a* fluorescence, which also indicate a more reduced state of the PQ pool in the *ics1* mutant (Fig. 3a, Table 1).

Changes in the redox status of the PQ pool also affect expression of chloroplast- and nuclear-encoded genes (Escoubas *et al*., 1995; Karpinski *et al*., 1997, 1999; Pfannschmidt *et al*., 1999, 2001, 2009; Muhlenbock *et al*., 2008). These changes may adjust PSI and PSII stoichiometry in response to PSI- or PSII-favouring light (Pfannschmidt *et al*., 2009; Rochaix, 2011) or may induce expression of genes encoding ROS-scavenging enzymes when the plants are exposed to excess light (Karpinski *et al*., 1997, 1999) and immune defence-related genes (Mullineaux *et al*., 2000; Muhlenbock *et al*., 2008). Here it was shown that nuclear-encoded genes induced in the *ics1* mutant encoded proteins predominantly targeted toward the chloroplasts (Fig. 5a, b). This supports the hypothesis that ICS1 is important for optimal photosynthesis (Mateo *et al*., 2006), and probably affects the whole cell through chloroplast to nucleus retrograde signalling dependent on the redox state of PQ pool (Figs 4, 5).

To test if the observed changes in the ST processes are connected with altered stoichiometry of the photosystems,

the chlorophyll *a*/*b* ratio was measured (Pfannschmidt *et al*., 2001). Chlorophyll *a*/*b* was decreased in *ics1* when compared with Col-0 (Table 1), which suggests that the PSII/PSI ratio is increased in *ics1*. PSI can only be located in unstacked thylakoids and at the ends of the thylakoid stacks, while PSII is located only in stacked grana (Dekker and Boekema, 2005). The increased level of PSII in relation to PSI in *ics1* was further confirmed by the presence of higher numbers of stacked grana in *ics1* (Fig. 2). On the other hand, the increased number of grana in *ics1* can be explained by inhibited ST. During the state 1 to state 2 transition, thylakoid membrane remodelling occurs and results in the unstacking of layers in the grana. This process involves breakage of the connections between the layers in the grana domains, thus reducing the number of layers in the grana (Chuartzman *et al*., 2008). In the present experiment, the transmission electron microscopy samples were prepared from state 2-favouring conditions (low light, short photoperiod). The increased number of layers in *ics1*, in comparison with the Col-0 grana (Fig. 2), can be explained by the inhibited unstacking of grana when the *ics1* plants are placed in state 2-favouring conditions.

The role of phylloquinone in the regulation of STs is unequivocal, but the mechanism of this process is still unknown. The results of the present experiments do not allow the exclusion of the role of the structural changes in PSI, leading to a steric obstacle for LHCII, or the higher reduction of the PQ pool, which is commonly known as a regulator of ST. Nevertheless, the results demonstrate that plant light acclimatory and immune defence responses are genetically, molecularly, physiologically, and biochemically linked to the functions of ICS1. These results have important implications for understanding how a plant's immune defences have evolved and for understanding a plant's biotic and abiotic integrated environmental stress response strategies. Therefore, the results may help in the development of the smart amelioration of plant performance under multivariable environmental conditions.

Supplementary data

Supplementary data are available at *JXB* online.

Figure S1. Light curves of various photosynthetic parameters in the WT and *ics1* mutant.

Figure S2. PSI activity in the WT and *ics1* mutant.

Acknowledgements

We thank Jean-Pierre Métraux and Floriane L'Haridon (University of Fribourg) for NahG seeds, and Ewa Niewiadomska and Zbigniew Miszalski (Institute of Plant Physiology, Polish Academy of Sciences) for help with Dual-Pam measurements. This research was supported by the Welcome2008/1 grant operated within the framework of the Foundation for Polish Science, co-financed by the European Regional Development Fund and by the REGPOT project FP7-286093 WULS-PLANT HEALTH.

References

Allen JF. 2003. State transitions—a question of balance. *Science* **299,** 1530–1532.

An C, Mou Z. 2011. Salicylic acid and its function in plant immunity. *Journal of Integrative Plant Biology* **53,** 412–428.

Apel K, Hirt, H. 2004. Reactive oxygen species: metabolism, oxidative stress, and signal transduction. *Annual Review of Plant Biology* **55,** 373–399.

Asada K. 1999. The water–water cycle in chloroplasts: scavenging of active oxygens and dissipation of excess photons. *Annual Review of Plant Physiology and Plant Molecular Biology* **50,** 601–639.

Aviv DH, Rustérucci C, Holt BF, Dietrich RA, Parker JE, Dangl JL. 2002. Runaway cell death, but not basal disease resistance, in lsd1 is SA- and NIM1/NPR1-dependent. *The Plant Journal* **29,** 381–391.

Baker NR. 2008. Chlorophyll fluorescence: a probe of photosynthesis *in vivo*. *Annual Review of Plant Biology* **59,** 89–113.

Behringer C, Bartsch K, Schaller A. 2011. Safeners recruit multiple signalling pathways for the orchestrated induction of the cellular xenobiotic detoxification machinery in Arabidopsis. *Plant, Cell and Environment* **34,** 1970–1985.

Bellafiore S, Barneche F, Peltier G, Rochaix JD. 2005. State transitions and light adaptation require chloroplast thylakoid protein kinase STN7. *Nature* **433,** 892–895.

Bonardi V, Pesaresi P, Becker T, Schleiff E, Wagner R, Pfannschmidt T, Jahns P, Leister D. 2005. PSII core phosphorylation and photosynthetic long-term acclimation require two different kinases in *Arabidopsis thaliana*. *Nature* **437,** 1179–1182.

Brautigam K, Dietzel L, Kleine T, *et al.* 2009. Dynamic plastid redox signals integrate gene expression and metabolism to induce distinct metabolic states in photosynthetic acclimation in Arabidopsis. *The Plant Cell* **21,** 2715–2732.

Chen H, Xue L, Chintamanani S, *et al.* 2009. ETHYLENE INSENSITIVE3 and ETHYLENE INSENSITIVE3-LIKE1 repress SALICYLIC ACID INDUCTION DEFICIENT2 expression to negatively regulate plant innate immunity in Arabidopsis. *The Plant Cell* **21,** 2527–2540.

Chow WS, Melis A, Anderson JM. 1990. Adjustments of photosystem stoichiometry in chloroplasts improve the quantum efficiency of photosynthesis. *Proceedings of the National Academy of Sciences, USA* **87,** 7502–7506.

Chuartzman SG, Nevo R, Shimoni E, Charuvi D, Kiss V, Ohad I, Brumfeld V, Reich Z. 2008. Thylakoid membrane remodeling during state transitions in Arabidopsis. *The Plant Cell* **20,** 1029–1039.

Clarke SM, Mur LAJ, Wood JE, Scott IM. 2004. Salicylic acid dependent signaling promotes basal thermotolerance but is not essential for acquired thermotolerance in Arabidopsis thaliana. *The Plant Journal* **38,** 432–447.

Coll NS, Epple P, Dangl JL. 2011. Programmed cell death in the plant immune system. *Cell Death and Differentiation* **18,** 1247–1256.

Damkjaer JT, Kereïche S, Johnson MP, Kovacs L, Kiss AZ, Boekema EJ, Ruban AV, Horton P, Jansson S. 2009. The photosystem II light-harvesting protein Lhcb3 affects the macrostructure of photosystem II and the rate of state transitions in Arabidopsis. *The Plant Cell* **21,** 3245–3256.

Dekker JP, Boekema EJ. 2005. Supramolecular organization of thylakoid membrane proteins in green plants. *Biochimica et Biophysica Acta* **1706,** 12–39.

Depège N, Bellafiore S, Rochaix JD. 2003. Role of chloroplast protein kinase Stt7 in LHCII phosphorylation and state transition in Chlamydomonas. *Science* **299,** 1572–1575.

Ducruet JM. 2003. Chlorophyll thermoluminescence of leaf discs: simple instruments and progress in signal interpretation open the way to new ecophysiological indicators. *Journal of Experimental Botany* **54,** 2419–2430.

Ducruet JM, Vass I. 2009. Thermoluminescence: experimental. *Photosynthesis Research* **101,** 195–204.

Escoubas JM, Lomas M, LaRoche J, Falkowski PG. 1995. Light intensity regulation of cab gene transcription is signaled by the redox state of the plastoquinone pool. *Proceedings of the National Academy of Sciences, USA* **92,** 10237–10241.

Fragnière C, Serrano M, Abou-Mansour E, Métraux JP, L'Haridon F. 2011. Salicylic acid and its location in response to biotic and abiotic stress. *FEBS Letters* **585,** 1847–1852.

Frenkel M, Bellafiore S, Rochaix JD, Jansson S. 2007. Hierarchy amongst photosynthetic acclimation responses for plant fitness. *Physiologia Plantarum* **129,** 455–459.

Gaffney T, Friedrich L, Vernooij B, Negrotto D, Nye G, Uknes S, Ward E, Kessmann H, Ryals J. 1993. Requirement of salicylic acid for the induction of systemic acquired resistance. *Science* **261,** 754–756.

Garcion C, Lohmann A, Lamodière E, Catinot J, Buchala A, Doermann P, Métraux JP. 2008. Characterization and biological function of the ISOCHORISMATE SYNTHASE2 gene of Arabidopsis. *Plant Physiology* **147,** 1279–1287.

Genger RK, Jurkowski GI, Mcdowell JM, Lu H, Jung HW, Greenberg JT, Bent AF. 2008. Signaling pathways that regulate the enhanced disease resistance of Arabidopsis 'defense, no death' mutants. *Molecular Plant-Microbe Interactions* **21,** 1285–1296.

Gentleman C, Carey VJ, Bates DM, *et al.* 2004. Bioconductor: open software development for computational biology and bioinformatics. *Genome Biology* **5,** R80.

Gross J, Cho WK, Lezhneva L, Falk J, Krupinska K, Shinozaki K, Seki M, Herrmann RG, Meurer J. 2006. A plant locus essential for phylloquinone (vitamin K1) biosynthesis originated from a fusion of four eubacterial genes. *Journal of Biological Chemistry* **281,** 17189–17196.

Ichimura K, Casais C, Peck SC, Shinozaki K, Shirasu K. 2006. MEKK1 is required for MPK4 activation and regulates tissue-specific and temperature-dependent cell death in Arabidopsis. *Journal of Biological Chemistry* **281,** 36969–36976.

Inoue Y. 1996. Photosynthetic thermoluminescence as a simple probe of photosystem II electron transport. In: Amesz J, Hoff AJ, eds. *Biophysical techniques in photosynthesis* . Berlin: Springer, 93–107.

Karnovsky MJ. 1965. A formaldehyde–glutaraldehyde fixative of high osmolarity for use in electron microscopy. *Journal of Cell Biology* **27,** 137–138.

Karpinska B, Wingsle G, Karpinski S. 2000. Antagonistic effects of hydrogen peroxide and glutathione on acclimation to excess excitation energy in Arabidopsis. *IUBMB Life* **50,** 21–26.

Karpinski S, Escobar C, Karpinska B, Creissen G, Mullineaux PM. 1997. Photosynthetic electron transport regulates the expression of cytosolic ascorbate peroxidase genes in Arabidopsis during excess light stress. *The Plant Cell* **9,** 627–640.

Karpinski S, Gabrys H, Mateo A, Karpinska B, Mullineaux PM. 2003. Light perception in plant disease defence signalling. *Current Opinion in Plant Biology* **6,** 390–396.

Karpinski S, Reynolds H, Karpinska B, Wingsle G, Creissen G, Mullineaux P. 1999. Systemic signalling and acclimation in response to excess excitation energy in Arabidopsis. *Science* **284,** 654–657.

Karpinski S, Szechynska-Hebda M, Wituszynska W, Burdiak P. 2013. Light acclimation, retrograde signalling, cell death and immune defences in plants. *Plant, Cell and Environment* **36,** 736–44.

Kruk J, Karpinski S. 2006. An HPLC-based method of estimation of the total redox state of plastoquinone in chloroplasts, the size of the photochemically active plastoquinone-pool and its redox state in thylakoids of Arabidopsis. *Biochimica et Biophysica Acta* **1757,** 1669–1675.

Kruk J, Strzałka K, Schmid GH. 1994. Antioxidant properties of plastoquinol and other biological prenylquinols in liposomes and solution, *Free Radical Research* **21,** 409–416.

Laloi C, Stachowiak M, Pers-Kamczyc E, Warzych E, Murgia I, Apel K. 2007. Cross-talk between singlet oxygen- and hydrogen peroxide-dependent signaling of stress responses in Arabidopsis thaliana. *Proceedings of the National Academy of Sciences, USA* **104,** 672–677.

Li Z, Wakao S, Fischer BB, Niyogi KK. 2009. Sensing and responding to excess light. *Annual Review of Plant Biology* **60,** 239–260.

Loake G, Grant M. 2007. Salicylic acid in plant defence—the players and protagonists. *Current Opinion in Plant Biology* **10,** 466–472.

Mateo A, Funck D, Muhlenbock P, Kular B, Mullineaux PM, Karpinski S. 2006. Controlled levels of salicylic acid are required for optimal photosynthesis and redox homeostasis. *Journal of Experimental Botany* **57,** 1795–1807.

Mateo A, Muhlenbock P, Rusterucci C, Chang, CC-C, Miszalski Z, Karpinska B, Parker JE, Mullineaux PM, Karpinski S. 2004. LESION SIMULATING DISEASE 1 is required for acclimation to conditions that promote excess excitation energy. *Plant Physiology* **136,** 2818–2830.

Mishina TE, Zeier J. 2007. Pathogen-associated molecular pattern recognition rather than development of tissue necrosis contributes to bacterial induction of systemic acquired resistance in Arabidopsis. *The Plant Journal* **50,** 500–513.

Misra AN, Dilnawaz F, Misra M, Biswal AK. 2001. Thermoluminescence in chloroplasts as an indicator of alterations in photosystem 2 reaction centre by biotic and abiotic stresses. *Photosynthetica* **39,** 1–9.

Miyake C, Miyata M, Shinzaki Y, Tomizawa K. 2005. CO2 response of cyclic electron flow around PSI (CEF-PSI) in tobacco leaves—relative electron fluxes through PSI and PSII determine the magnitude of non-photochemical quenching (NPQ) of Chl fluorescence. *Plant and Cell Physiology* **46,** 629–637

Mullineaux PM, Ball L, Escobar C, Karpinska B, Creissen G, Karpinski S. 2000. Are diverse signalling pathways integrated in the regulation of arabidopsis antioxidant defence gene expression in

response to excess excitation energy? *Philosophical Transactions of the Royal Society B: Biological Sciences* **355,** 1531–1540.

Muhlenbock P, Szechynska-Hebda M, Plaszczyca M, Baudo M, Mullineaux PM, Parker JE, Karpinska B, Karpinski S. 2008. Chloroplast signaling and LESION SIMULATING DISEASE1 regulate crosstalk between light acclimation and immunity in Arabidopsis. *The Plant Cell* **20,** 2339–2356.

Munekage Y, Shikanai T. 2005. Cyclic electron transport through photosystem I. *Plant Biotechnology* **22,** 361–369.

Niewiadomska E, Bilger W, Gruca M, Mulisch M, Miszalski Z, Krupinska K. 2011. CAM-related changes in chloroplastic metabolism of Mesembryanthemum crystallinum L. *Planta* **233,** 275–285.

Niyogi KK. 1999. Photoprotection revisited: genetic and molecular approaches. *Annual Review of Plant Physiology and Plant Molecular Biology* **50,** 333–359.

Pfannschmidt T, Bräutigam K, Wagner R, Dietzel L, Schröter Y, Steiner, S Nykytenko A. 2009. Potential regulation of gene expression in photosynthetic cells by redox and energy state: approaches towards better understanding. *Annals of Botany* **103,** 599–607.

Pfannschmidt T, Nilsson A, Allen JF. 1999. Photosynthetic control of chloroplast gene expression. *Nature* **397,** 625–628.

Pfannschmidt T, Schütze K, Brost M, Oelmüller R. 2001. A novel mechanism of nuclear photosynthesis gene regulation by redox signals from the chloroplast during photosystem stoichiometry adjustment. *Journal of Biological Chemistry* **276,** 36125–36130.

Pribil M, Pesaresi P, Hertle A, Barbato R, Leister D. 2010. Role of plastid protein phosphatase TAP38 in LHCII dephosphorylation and thylakoid electron flow. *PLoS Biology* **8,** e1000288.

Rochaix JD. 2011. Regulation of photosynthetic electron transport. *Biochimica et Biophysica Acta* **1807,** 375–383.

Ruban A, Lavaud J, Rousseau B, Guglielmi G, Horton P, Etienne AL. 2004. The super-excess energy dissipation in diatom algae: comparative analysis with higher plants. *Photosynthesis Research* **82,** 165–175.

Sane PV, Ivanov AG. Öquist G, Hüner NPA. 2012. Thermoluminescence. In Eaton-Rye JJ, Tripathy BC, Sharkey TD (eds), *Photosynthesis: plastid biology, energy conversion and carbon assimilation*, Advances in Photosynthesis and Respiration volume 34. Dordrecht: Springer, PP. 445–474.

Shapiguzov A, Ingelsson B, Samol I, Andres C, Kessler F, Rochaix JD, Vener AV, Goldschmidt-Clermont M. 2010. The PPH1 phosphatase is specifically involved in LHCII dephosphorylation and state transitions in Arabidopsis. *Proceedings of the National Academy of Sciences, USA* **107,** 4782–4787.

Smyth GK. 2005. Limma: linear models for microarray data. In: Gentleman R, Carey V, Dudoit S, Irizarry R, Huber H, eds. *Bioinformatics and computational biology solutions using R and Bioconductor* . New York: Springer: 397–420.

Szechynska-Hebda M, Kruk J, Gorecka M, Karpinska B, Karpinski S. 2010. Evidence for light wavelength-specific systemic photoelectrophysiological signalling and cellular light memory of excess light episode in Arabidopsis. *The Plant Cell* **22,** 1–18.

Van Breusegem F, Bailey-Serres J, Mittler R. 2008. Unraveling the tapestry of networks involving reactive oxygen species in plants. *Plant Physiology* **147,** 978–984.

van Oostende C, Widhalm JR, Basset JC. 2008. Detection and quantification of vitamin K1 quinol in leaf tissues. *Phytochemistry* **69,** 2457–2462.

Vlot AC, Dempsey DA, Klessig DF. 2009. Salicylic acid, a multifaceted hormone to combat disease. *Annual Review of Phytopathology* **47,** 177–206.

Wildermuth MC, Dewdney J, Wu G, Ausubel FM. 2001. Isochorismate synthase is required to synthesize salicylic acid for plant defence. *Nature* **414,** 562–565.

Wilson CL, Miller CJ. 2005. Simpleaffy: a BioConductor package for Affymetrix quality control and data analysis. *Bioinformatics* **21,** 3683–3685.

Wituszynska W, Galazka K, Rusaczonek A, Vanderauwera S, Van Breusegem F, Karpinski S. 2013. Multivariable environmental conditions promote photosynthetic adaptation potential in Arabidopsis thaliana. *Journal of Plant Physiology* **170,** 548–559.